A STUDY OF CARRIER GENERATION IN, AND INTERACTION OF, SPACE-CHARGE REGIONS IN GERMANIUM

by

RONALD REID MITCHELL

B.A.Sc., University of British Columbia, 1957

A THESIS SUBMITTED IN PARTIAL FULFILMENT OF
THE REQUIREMENTS FOR THE DEGREE OF
MASTER OF APPLIED SCIENCE

in the Department
of
Physics

We accept this thesis as conforming to the
required standard

THE UNIVERSITY OF BRITISH COLUMBIA

September, 1959

ABSTRACT

Germanium space-charge regions have been studied under conditions of double-depletion achieved by applying a reverse bias to both junctions of a transistor structure. The generation and distribution of carriers between the two junctions are described in terms of models for the thermal generation of carrier pairs and for potential distribution in a cylindrical system.

Measurements over a wide range of temperature reveal that generation of carriers occurs through the medium of one or more sets of recombination centers and not by direct transition between the valence and conduction bands even at elevated temperatures. The Shockley-Read recombination-generation theory is applied to obtain the activation energies associated with the recombination centers.

The impurity density, base width and junction areas are estimated from measurements of punchthrough voltage and junction capacitance. For some specimens the capacitance measurements made with one junction floating confirm the sharp increase in capacitance at punchthrough noted by Barker.

The distribution of current between the junctions when both are equally reverse biased is found to be roughly proportional to their areas. It is also shown that control of the reverse current across one junction may be achieved by variation of the reverse-bias on the other junction. The mechanism of this interaction is considered in terms of the diffusion of carriers between the two space-charge regions.

The phenomen of slightly non-saturating reverse current is explained in terms of the expansion with reverse bias of the space-charge region within the base. An expression relating the base current and reverse bias in a cylindrical system shown to give good agreement with experiment for one specimen. For the units in which the increase in current with voltage is appreciable, space-charge expansion cannot account for the increase and two other mechanisms are considered: avalanche multiplication in the bulk and along the surface, and a high generation rate on the surface.

The surface conduction channels on the base region are investigated in two ways. Maximum floating junction potentials are calculated from measured values of the common emitter amplification factor (using the Shockley 1949 theory) and these are compared with directly measured potentials. A second method involves direct measurement of a.c. surface conductance between collector and emitter when both junctions are reverse-biased to prevent bulk conduction. Both tests reveal very small degrees of surface conductance on all specimens.

In presenting this thesis in partial fulfilment of the requirements for an advanced degree at the University of British Columbia, I agree that the Library shall make it freely available for reference and study. I further agree that permission for extensive copying of this thesis for scholarly purposes may be granted by the Head of my Department or by his representatives. It is understood that copying or publication of this thesis for financial gain shall not be allowed without my written permission.

Department of Physics

The University of British Columbia,
Vancouver 8, Canada.

Date Sept 22, 1959

TABLE OF CONTENTS

ILLUSTRATIONS

ACKNOWLEDGEMENTS

The author wishes to thank Professor R.E. Burgess for his guidance of this investigation and help in preparation of this thesis. Financial support in the form of a Defence Research Board grant is gratefully acknowledged.

CHAPTER I

INTRODUCTION

1.1 Double-Depletion in Reverse-Biased Transistors

Double-depletion in pnp and npn junction transistors occurs when both junctions are reverse-biased so that the space charge regions normally present at thermal equilibrium are extended into the base. In this circumstance there is no injection of carriers into the base region and the current across the junction is due almost entirely to carriers thermally generated in the base. If sufficiently large reverse biases are applied the two space charge regions will meet after which a further increase in the reverse bias of one junction will cause the space-charge region of that junction to extend across the base ultimately reaching the opposite junction - a condition known as "punchthrough". At punchthrough there is a continuous potential gradient between the two junctions and a current due to injection of carriers from the less biased junction will flow between them. With further increase in the variable reverse bias this current will increase rapidly to tend to keep the voltage drop across the space-charge regions constant. If, however, the two reverse biases are kept equal and increased, punchthrough will not occur; there will be only a slow change in the currents across the junctions until the occurence of break-down characterized by a rapid increase in current.

SPACE-CHARGE AND POTENTIAL DISTRIBUTION

IN THE BASE REGION

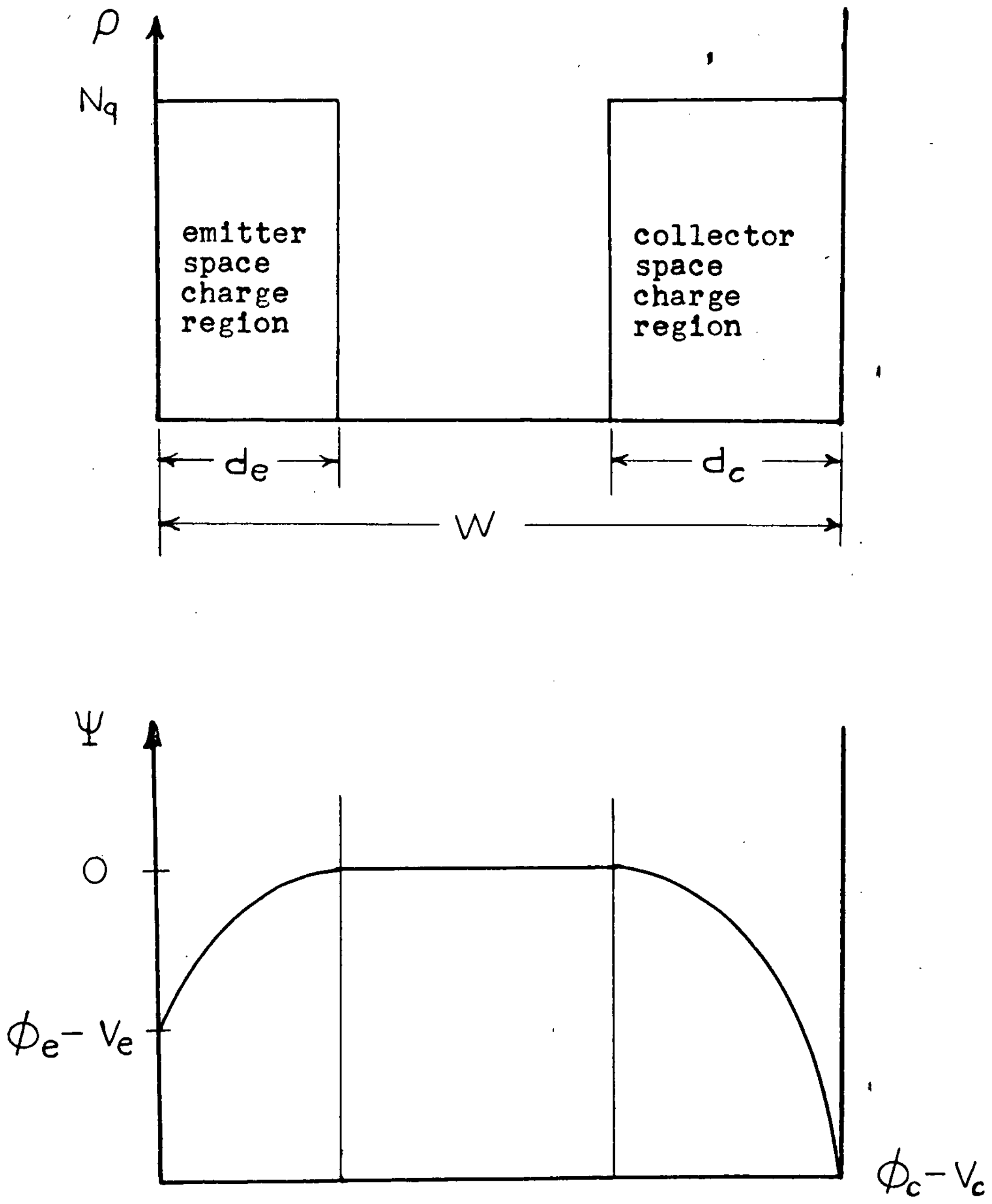

FIG. 1

This work is concerned with three points of fundamental interest in the study of the interaction of the two depletion regions: the characteristics of the collector and emitter currents before punchthrough, the mechanism of hole-electron pair generation in the base, and the mechanism of breakdown. Relevant previous theoretical and experimental investigations are summarized in the remainder of this chapter. The three succeeding chapters describe experimental work on selected transistors and correlate the results with existing theory. The final chapter consists of a summary of the work and a description of a simple model which agrees with the experimental results.

1.2 Potential and Space-charge Distributions for an Idealized Transistor.

Figure 1 shows the potential and space-charge distributions under the condition of double depletion for an idealized one-dimensional pnp transistor. The built-in potential steps at the junctions are neglected as small compared to the applied reverse biases. In order to have zero net charge in a junction, the ratio of the widths of the space-charge regions in the p- and n-type materials must be in the inverse ratio of their impurity ion densities. Here the n-type resistivity is much greater so the expansion of the space-charge region into the p-type material may be neglected. It is further assumed that the boundaries of the space-charge regions are abrupt whereas for a real junction they are spread over one Debye length, L_d, where

$$L_d = \sqrt{\epsilon kT/4\pi q^2 N} \qquad 1.2.1$$

and ϵ = permitivity, k = Boltzmann's constant, q = electronic charge, and N = impurity ion density in the base.

The potential distribution is obtained by a simple double integration of Poisson's equation under the boundary conditions that the potential be equal to the applied biases at the junctions and zero within the undepleted region of the base. The width of the space-charge region for each junction is found to be

$$d_e = \sqrt{\frac{(\phi_e - V_e)}{2\rho}}, \qquad d_c = \sqrt{\frac{(\phi_c - V_c)}{2\rho}} \qquad 1.2.2$$

where ρ is the space charge density, and ϕ_e, ϕ_c the built-in biases at the emitter and collector and V_e, V_c the magnitudes of the applied bias at the junctions. In the case of a single space-charge layer, punchthrough will occur at the emitter-collector potential drop given by

$$V_p = \frac{2\rho w^2}{\epsilon} \qquad 1.2.3$$

At punchthrough a short-circuit path exists between emitter and collector and the collector and emitter bias voltages will remain locked together, that is

$$|V_c - V_e| = V_p \qquad 1.2.4$$

CURRENT VOLTAGE CONVENTIONS

FOR A PNP TRANSISTOR

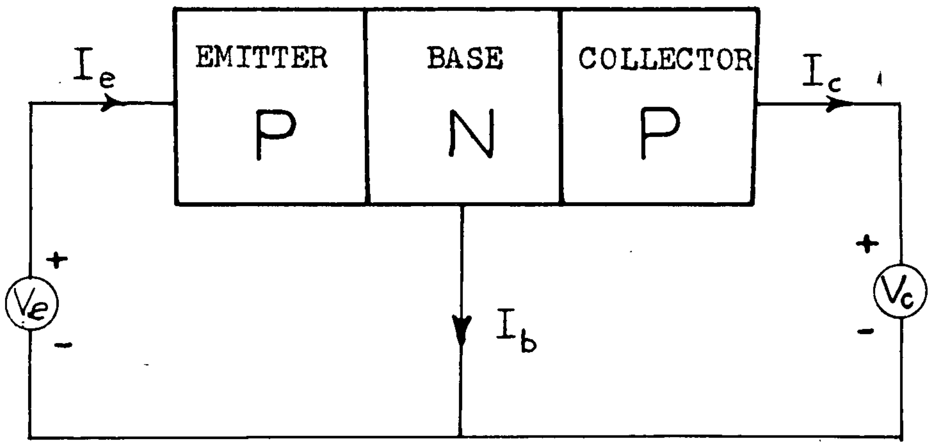

FIG. 2

From figure 1 it may be seen that complete depletion of the base corresponds to a potential distribution in which the two parabolic segments unite to form a single parabola. The voltage relationship is then

$$\sqrt{\phi_e - V_e} + \sqrt{\phi_c - V_c} = \sqrt{V_p} \qquad 1.2.5$$

The presence of the ionic charge Q = NqAd in a depletion layer results in a dynamic capacitance measured between base and either collector or emitter of

$$C = \frac{dQ}{dV} = A \frac{Nq\epsilon}{2(V + \phi)} \qquad 1.2.6$$

or geometrically

$$C_{eb} = \frac{\epsilon A}{d_e} \qquad C_{cb} = \frac{\epsilon A}{d_c} \qquad 1.2.7$$

where A is the cross-sectional area of the ideal planar diode and d_e and d_c refer to the widths of the corresponding space charge regions.

1.3 Minority-Carrier Diffusion Current Relations

The theory of current flow developed by Shockley (1949) can be applied to the model described above if we make the assumptions of non-degenerate distributions for electrons and holes and long bounding p regions. With the current and voltage conventions shown in figure 2 Shockley's equations are:

$$I_e = \frac{AqD_p p_n}{L_p}\left[\coth \frac{w}{L}(e^{\frac{qV_e}{KT}} - 1) - \operatorname{csch}(e^{\frac{qV_c}{KT}} - 1)\right] \qquad 1.3.1$$

$$I_c = \frac{-AqD_p p_n}{L_p}\left[\coth \frac{w}{L}(e^{\frac{qV_c}{KT}} - 1) - \operatorname{csch}(e^{\frac{qV_e}{KT}} - 1)\right] \qquad 1.3.2$$

where q = electronic charge, p_n = thermal equilibrium concentration of holes in the base and D_p = hole diffusion constant.

For double depletion both V_e and V_c are negative so there will be no hole injection. The two components of each current reach saturation values when the reverse biases exceed a few times kT/q. When w is within an order of magnitude of L, the first term in the expressions for I_e and I_c will dominate and the reverse currents will be virtually independent of the bias at the other junction. However, as was pointed out by Early (1952) the widening of the space charge layers will reduce the effective width of the base, and thus some control of the collector current by variation of emitter bias becomes possible. Stafayev, Tuchkevich and Yakovchuck (1956) have shown that operation of reverse biased transistors as amplifiers is possible if the effective base width can be decreased to the magnitude of L before the currents are fully saturated. The requirements for achieving useful amplifications are: a high operating temperature to provide a large number of thermally generated minority carriers in the base, a narrow base width so that the effective base width will

BASIC TRANSITION PROCESSES

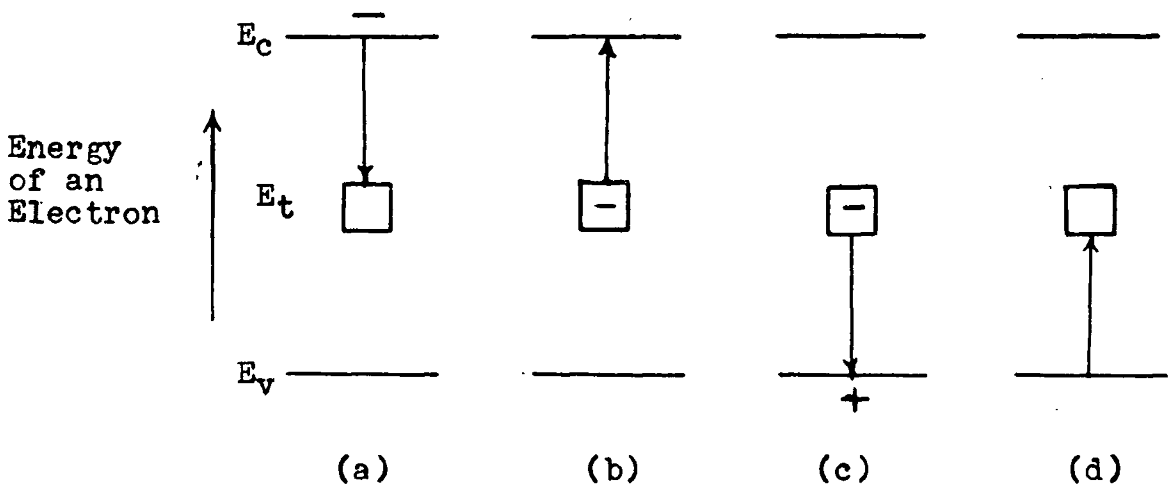

Arrows denote electron transition.

(a) electron capture, (b) electron emission,
(c) hole capture, (d) hole emission

FIG. 3

be small before the reverse currents have saturated, and low impurity density in the base in order that the depletion regions will expand into the base rather than into the emitter and collector.

1.4 Mechanisms of Carrier Generation in Base

The saturation currents across the junctions may arise through several mechanisms. Most important of these are bulk and surface generation of carriers. There may also be some current due to hole injection by the contacts to the base. Creation of hole-electron pairs in the bulk of the base may occur either by direct transitions of electrons from the valence to the conduction band or through the medium of recombination centres having energy levels in the forbidden zone. These centers arise from defects of a chemical or physical nature in the crystal lattice.

Shockley and Read (1952) have used a statistical approach to derive the recombination rates in the body of a non-degenerate semiconductor having a single trap level. Carrier recombination and generation are considered to proceed by means of the four basic processes illustrated in figure 3, at rates determined by the availability of holes and electrons and the densities of occupied and unoccupied centers. Under equilibrium conditions the rates of hole and electron emission are equal to the rates of hole and electron capture respectively, and under steady state conditions the net rate of electron capture is equal to the net rate of hole capture.

With these assumptions Shockley and Read find the net recombination rate per unit volume to be

$$r - g \equiv U = \frac{pn - n_i^2}{(n - n_1)\tau_{po} + (p - p_1)\tau_{no}} \qquad 1.4.1$$

where n = density of electrons in the conduction band, p = density of holes in the valence band, n_1 (p_1) = density of electrons (holes) in the conduction (valence) band when the Fermi level falls at the trap level, τ_{po} = lifetime for holes in highly n-type material, τ_{no} = lifetime for electrons in highly p-type material, and n_i = density of holes or electrons in an intrinsic specimen.

In a space charge region the carriers are swept out before they can recombine consequently the generation rate for hole-electron pairs becomes

$$g_{s.c.} = \frac{n_i^2}{\tau_{po}\, n_1 + \tau_{no}\, p_1} \qquad 1.4.2$$

An analysis of surface recombination has been carried out by Brattain and Bardeen (1952) along lines similar to the above treatment. In their model, surface states replace the recombination centers present in the bulk. Surface recombination is more difficult to investigate as there is almost certainly more than one trap level.

1.5 Non-saturating Reverse Currents

For an ideal transistor under conditions of double depletion the base current will be constant over the range between a few times kT/q and the onset of breakdown. However, in most pn junctions the reverse current increases with increasing bias. This was originally attributed to surface leakage, but in cases where the space charge generated current predominates an additional voltage dependence may exist due to expansion of the space charge region with increasing reverse bias.

The latter type of voltage dependence has been investigated by Sah, Noyce and Shockley (1956). They have shown that the space charge generated current will tend to dominate in transistors in the case of short lifetimes, low resistivities and large energy gaps. For a step-junction with a reverse bias over a few times kT/q the generation rate will be virtually constant throughout the space charge region so the reverse saturation current will increase as the square root of the applied reverse bias.

Brown (1952) has studied surface leakage via areas of n-type conductivity on the surface of p-type germanium. In his theory he proposes that previous chemical and electrical treatment has resulted in a layer of positive charge on the surface of the p-type material. Electrical neutrality then requires a net deficit of negative charge within the crystal and thus there arises an inversion layer just below the surface, in which there is an excess of electrons. These electrons provide a surface conducting path or "channel". Later experiments (Christensen 1954) have revealed the p-TYPE SURFACE CHANNEL ON n-TYPE BASE REGION

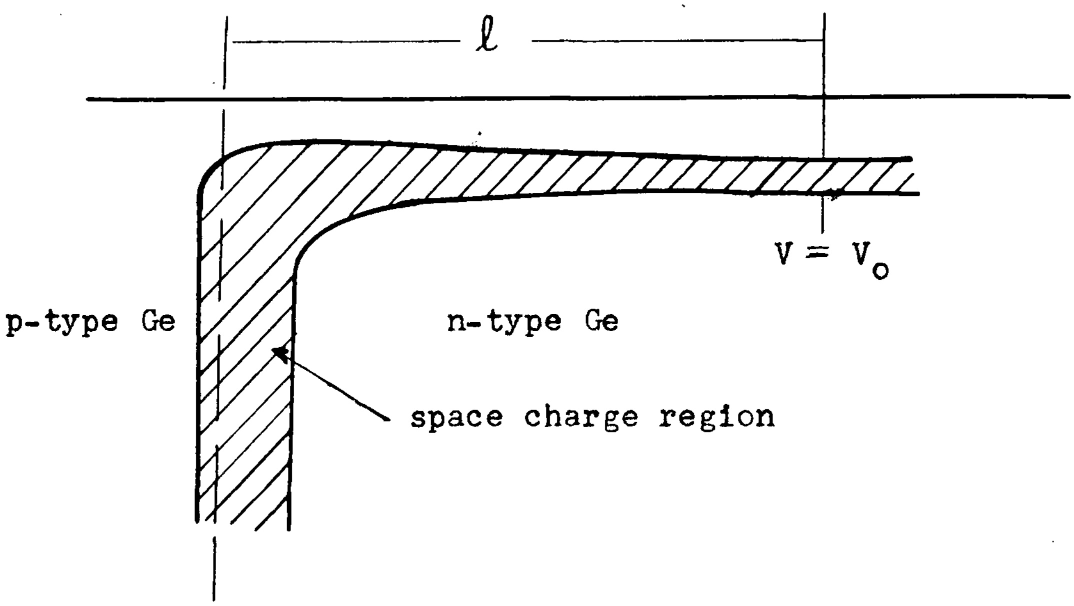

ℓ = channel length

FIG. 4

occurrence of p-type channels on n-type germanium.

The Brown model has been extended by McWhorter and Kingston (1954). They assert that the channel forms an extension of the normal reverse-biased junction as shown in figure 4. There will be an increase in reverse current due to bulk generated electrons and surface generated holes being swept into the channel. The current flowing in the channel causes a voltage drop along its length; the effective length of the channel over which it collects carriers extends from the junction to the point at which the voltage in the channel is equal to the thermal energy of the carriers, kT/q. Taking the surface resistance of the channel as proportional to the applied voltage, McWhorter and Kingsley deduced that for the junction of figure 4, the excess reverse saturation current would vary as $(\ln V/V_0)^{\frac{1}{2}}$ where V is the applied bias and V_0 the voltage at the extreme of the effective length of the channel.

1.6 Breakdown Mechanisms

Two distinct mechanisms have been advanced to account for the sharp rise in the current-voltage characteristic of a reverse biased junction. According to the Zener breakdown theory the rapid increase of current with voltage is due to the direct excitation of electrons from the valence to the conduction band under the influence of a strong electric field. The avalanche breakdown mechanism is analogous to Townsend discharge in gases. The electrons or holes gain sufficient energy in the high field region to cause impact ionization of the neutral atoms. The electron-hole pairs thus formed in turn produce other carrier pairs and a multiplicative process ensues.

The form of the current voltage characteristic at breakdown serves to determine which mechanism is responsible. Zener breakdown occurs abruptly when a certain critical field is reached somewhere in the semiconductor. Whereas in avalanche breakdown current multiplication commences before Zener breakdown. In the case of avalanche breakdown the application of reverse bias will widen the area of the junction and increase the probable number of ionizing collisions. The extent to which the reverse bias widens the junction area is dependent on the impurity density; thus extent of avalanche multiplication is dependent on impurity density while the field for Zener breakdown is not.

The form of the reverse current characteristic before breakdown when the avalanche mechanism is operative is obtained by multiplying the saturation current by an empirical factor due to Miller (1955):

$$M(V) = \frac{1}{1 - (V/V_B)^3} \qquad 1.6.1$$

where V_B is the breakdown voltage which in Ge is given approximately by

$$V_B = 10^{13} N^{-0.728} \qquad 1.6.2$$

CHARACTERISTICS OF TRANSISTORS

TRANSISTOR	13	21	46
TYPE	2N137	2N137	2N137
V_p	12 v	7 v	14 v
BASE WIDTH	$1.3\text{x}10^{-3}$ cm	$1.3\text{x}10^{-3}$ cm	$1.3\text{x}10^{-3}$ cm
A_e	0.0021 cm^2	0.0060 cm^2	0.0040 cm^2
A_c	0.0044 cm^2	0.0030 cm^2	0.0073 cm^2
N_I	$3.0\text{x}10^{+14}$ cm^{-3}	$1.0\text{x}10^{14}$ cm^{-3}	$1.4\text{x}10^{14}$ cm^{-3}
V_B	328 v	795 v	608 v

TABLE 1

Zener breakdown need not be considered in interpreting the results of this work. Miller has shown that very high fields are required for Zener breakdown - greater than 320 kv cm^{-1} in germanium.

Miller has pointed out that surface breakdown may occur at voltages lower than bulk breakdown voltage. Brattain and Garrett have investigated this phenomena. Their results indicate that surface breakdown like bulk breakdown is multiplicative, and that it will occur at voltages lower than bulk breakdown voltage if the surface charge is the same sign as that of the fixed body impurity on the high resistivity side of the junction.

CIRCUIT FOR MEASUREMENT OF FLOATING

EMITTER POTENTIALS

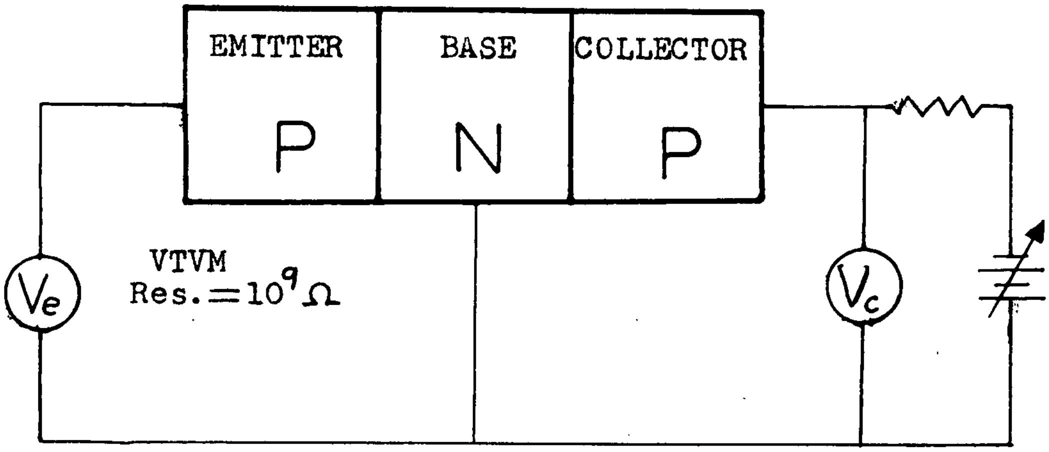

FIG. 5

CHAPTER II

CARRIER GENERATION IN THE BASE REGION

2.1 Characteristics of Transistors Investigated

The transistors used in the investigation were chosen from commercially available germanium fused junction, high frequency units. The thin base of high frequency types generally results in a punchthrough voltage lower than the breakdown voltage, and a fused junction comes nearer than a diffused junction to providing the step junction of the theory.

Several parameters which are useful in the selection of units for various measurements and in the evaluation of results may be obtained by measurement or calculated from the manufacturer's specifications. These are listed for three units in Table 1.

The base widths were obtained from the manufacturer's alpha-cutoff frequency and the formula

$$f = \frac{0.4\ D_p}{w^2} \qquad 2.1.1$$

The punchthrough voltages were measured in the circuit of fig. 5 devised by Schenkel and Statz (1954). V_p is indicated by a sharp increase in the floating potential of the open circuited junction as the reverse bias on the other junction is increased.

The emitter and collector areas were obtained from measurements of junction capacity at punchthrough as described

FLOATING EMMITER POTENTIALS AND CONDUCTANCES

TRANSISTOR	TYPE	MEASURED β	MEASURED V_f (volts)	V_f (calc.) $= \frac{KT}{q} \ln(1+\beta)$	g (mhos)
13	2N123	47	0.075	0.095	0.0032
21	2N137	27	0.10	0.080	
39	2N137	40	0.135	0.094	0.0011
46	2N137	31	0.068	0.088	0.0056
12	2N123	54	0.107	0.101	0.0009

TABLE 2

in section 2.3, and the expression for geometrical capacity in equation 1.1.6.

The bulk breakdown voltages were calculated from the empirical equation of Miller (1956)

$$V_B = 1.0 \times 10^{13} N_I^{-0.725} \qquad 2.1.2$$

where N_I is the impurity density in the base region.

2.2 Tests for Surface Conduction

Since the theory outlined in the introduction is based on bulk properties of the base region, the units used in the investigation must be chosen to be as free as possible from surface conduction channels between the collector and emitter. These can be detected (i) indirectly by measurement of the maximum floating emitter potential when the collector junction is reverse biased below punchthrough or (ii) directly by measurement of the ac conductance between emitter and collector when both junctions are reverse biased to prevent bulk conduction.

From equation 1.3.2, when I_e 0 the maximum floating emitter potential is

$$V_f = \frac{kT}{q} \ln(1-\alpha) \qquad 2.2.1$$

where $\alpha = \operatorname{sech} \frac{w}{L}$ is the common-base current gain. Brown (1953) found that the presence of surface channels leads to a floating emitter potential several times this value.

CIRCUIT FOR MEASUREMENT OF β

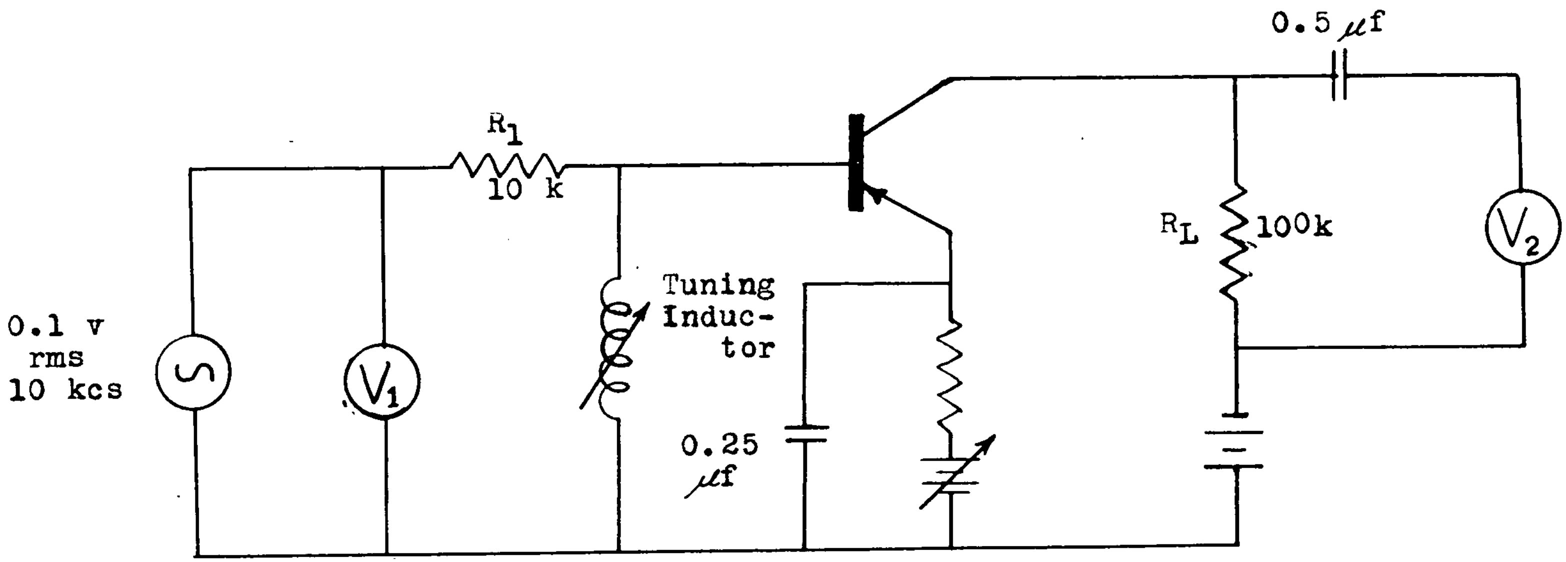

FIG. 6

Specimens of four different types of transistor were tested in the circuit of figure 5, and the measured floating emitter potentials were first compared with those calculated from the manufacturer's value of alpha. In all cases the measured values were slightly lower than those calculated indicating that the actual alpha's were lower than those specified. Alpha's for the individual transistors were therefore obtained experimentally using the circuit of fig. 6 which measures common emitter current gain as

$$\beta = \frac{V_2/R_L}{V_1/R_1} \qquad 2.2.2$$

if R_L is small compared with the output impedance of the transistor and R large compared with the input impedance. β is related to α by

$$\alpha = \frac{\beta}{1 + \beta} \qquad 2.2.3$$

Measurements were made at a frequency of 10 kc. The values of β thus obtained are necessarily inaccurate because at high frequency the emitter capacity shunts the input current. The purpose of the high impedance coil is to reduce this inaccuracy by tuning the emitter capacity. However, emitter capacity varies from unit of unit, and the finite resistance of the coil necessitates readjustment of the supply voltage; hence this is not a fixed condition test.

The values of V_f calculated from the measured alpha's are in most cases slightly lower than measured. Measured

CIRCUIT FOR MEASUREMENT OF SURFACE CONDUCTANCE

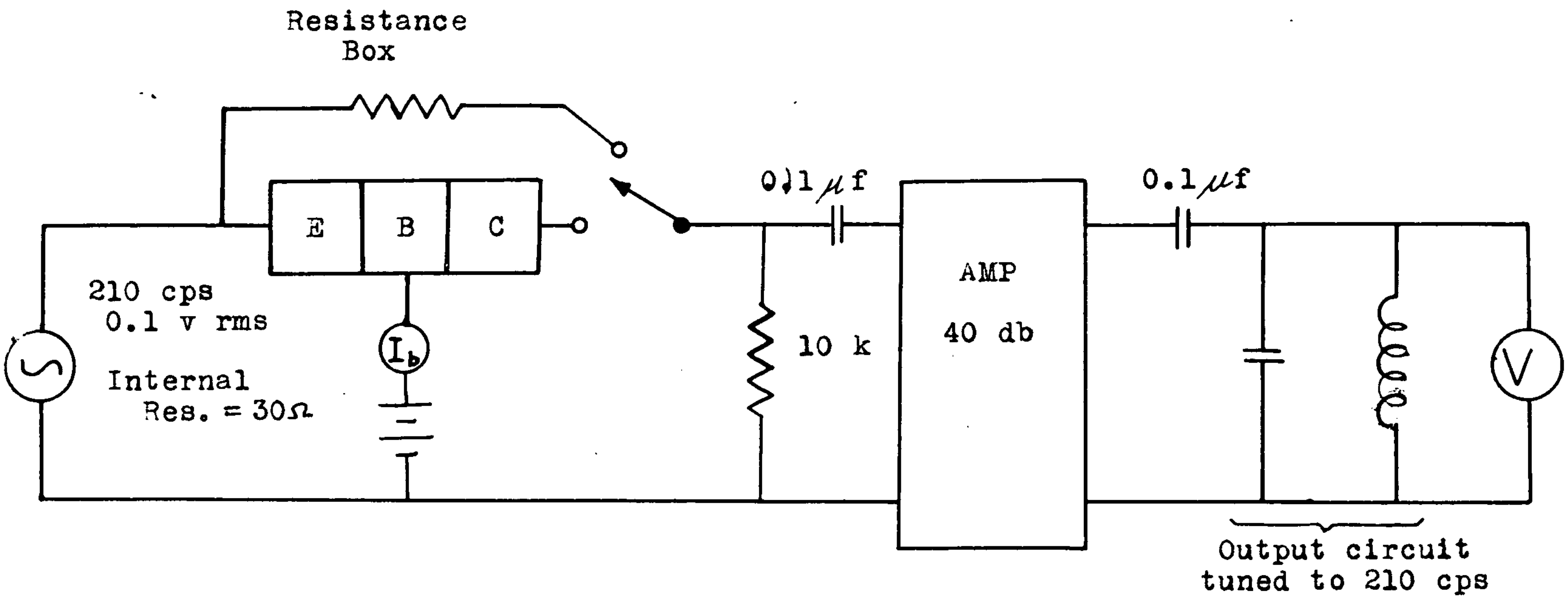

FIG. 7

and calculated values are compared in Table 2.

A method of measuring surface conductivity which is more directly quantitative than the Brown test is that of Statz, de Mars, and Davis (1958). The two junctions are provided with a common reverse bias to prevent bulk conduction as shown in fig. 7, and an ac signal is injected into the emitter-base circuit. The conducting path provided by the surface channels is replaced by a resistance box and the resistance adjusted to produce the same voltage at the output of the tuned amplifier. The disadvantages of this method are that for very low conductances noise may obscure the signal, and the reverse biasing may precipitate surface breakdown with a consequent multiplication of carriers and increase in conductance as is probably the case with specimens 46 and 13.

2.3 Capacitance Characteristics

The differential capacities of reverse biased junctions were measured in several transistors using the circuit of figure 8. Not only do these measurements allow an estimate of the junction areas and impurity densities, but also provide criteria of uniform impurity density and planar geometry, for, in this case, from equation 1.6.1, a plot of ln C vs ln V should yield a straight line of slope $-\frac{1}{2}$ when $V \gg \phi$.

The curves shown in fig. 9 were characteristic of two transistors. Others did not show the sharp increase in

CIRCUIT FOR MEASUREMENT OF JUNCTION CAPACITANCE

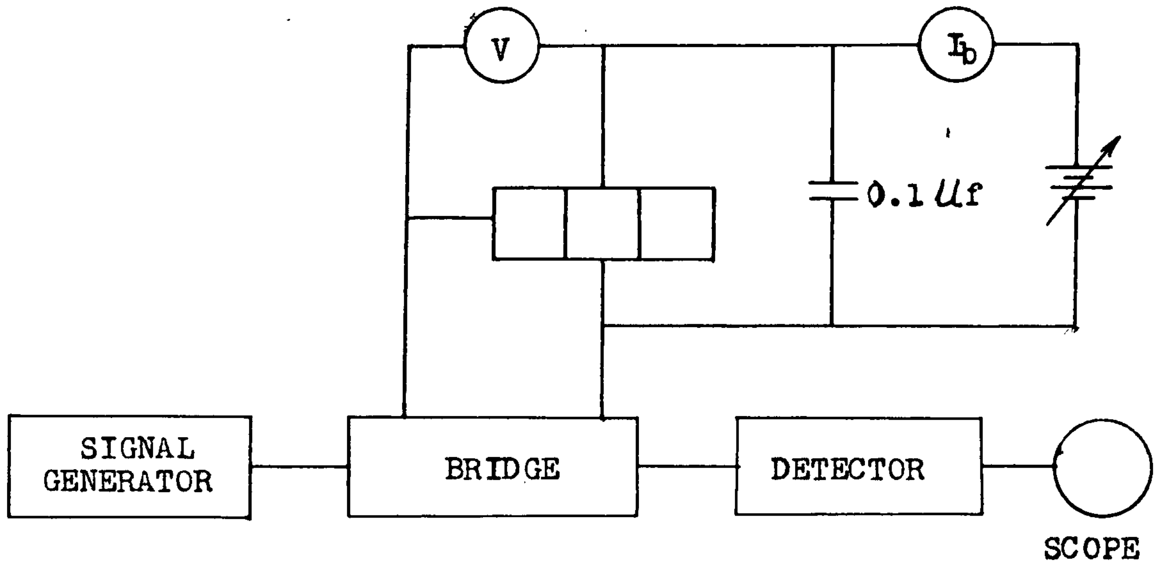

FIG. 8

JUNCTION CAPACITANCE CURVES

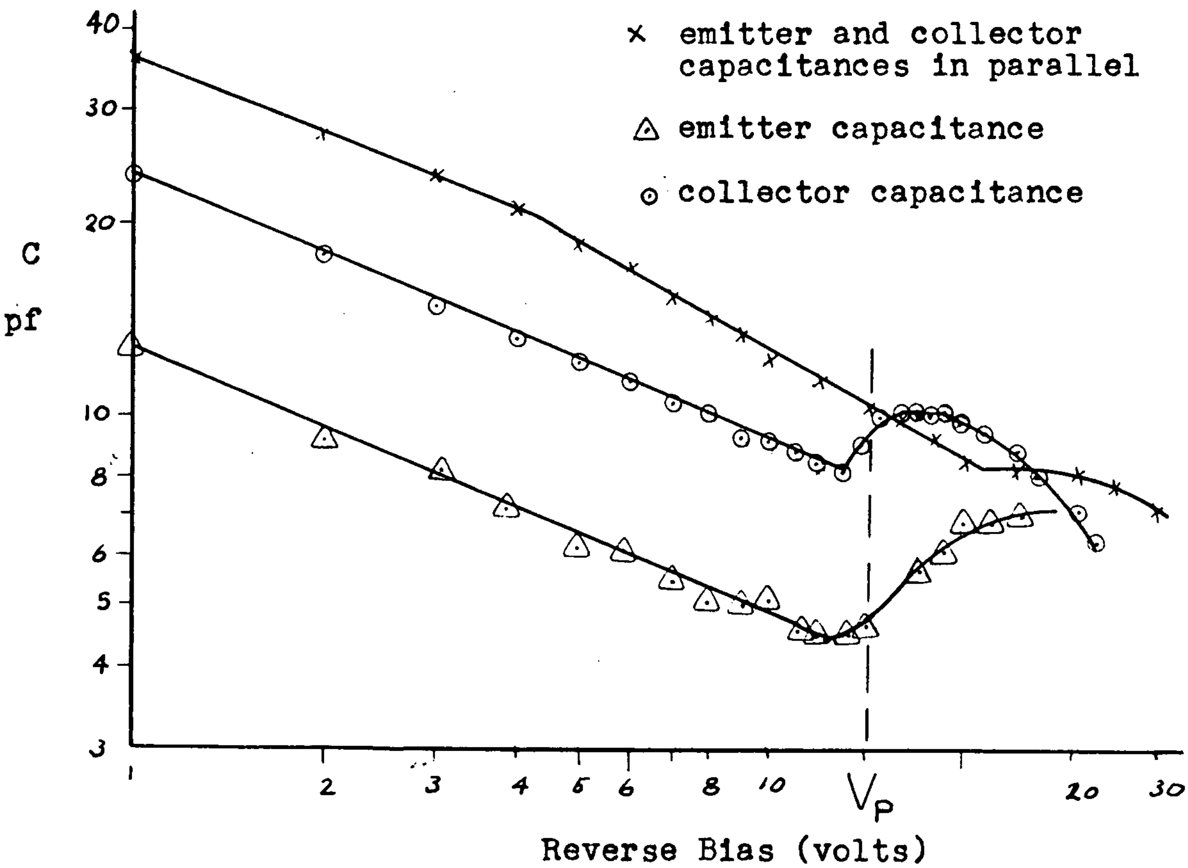

FIG. 9

collector and emitter junction capacities at punchthrough. All gave slopes of around -0.35.

The sharp increase in junction capacity at punchthrough was first noted by Barker (1956). His explanation is that the real geometry of a transistor is spherical rather than plane and when as in fig. 10b the expanding collector space charge region just touches the emitter space charge region, the emitter capacitance is suddenly shunted into the collector circuit.

Those specimens exhibiting the Barker effect were those that showed low breakdown voltages with "soft" breakdown characteristics. Perhaps in the Barker effect transistors the low conductance associated with incipient breakdown results in a low resistance path between the two space charge regions when their outer boundaries just touch, while in the non-Barker transistors a low resistance contact is not established until the two regions have overlapped to the extent of a Debye length at which point the emitter space charge will not have much external area.

2.4 Activation Energies

The generation rate of carrier pairs via recombination centers in a space charge region is, from equation 1.4.2

$$g = \frac{n_i^2}{\tau_{po}\, n_1 + \tau_{no}\, p_1} \qquad 2.4.1$$

where

THREE DIMENSIONAL MODEL OF A PNP TRANSISTOR
UNDER VARIOUS BIASING CONDITIONS

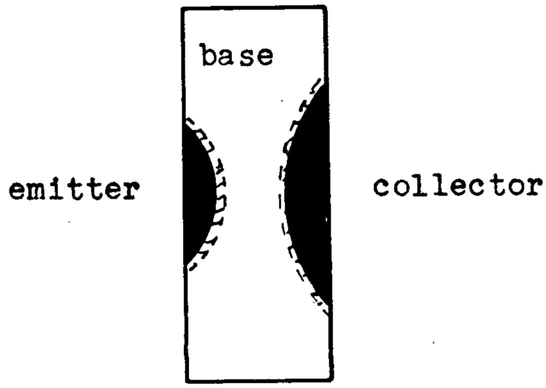

 Depleted Region

(a) Unbiased

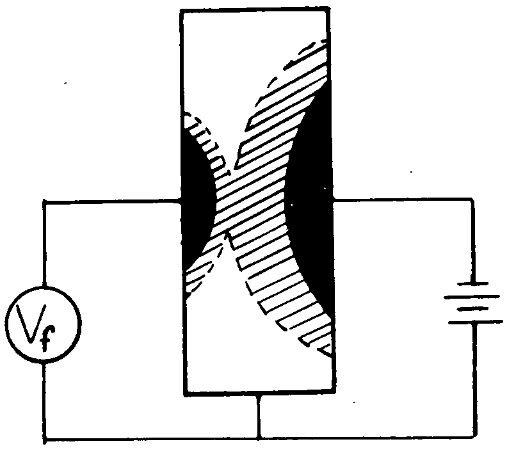

(b) At punchthrough

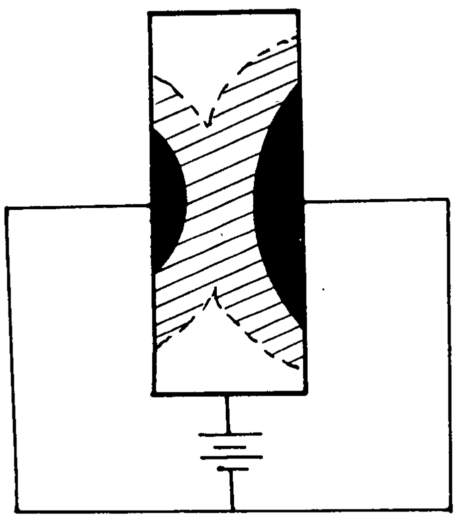

(c) Double-depletion

FIG. 10

$$n_1 = 2\left(\frac{2\pi m_e\, kT}{h^2}\right)^{3/2} \exp -\left(\frac{E_c - E_t}{kT}\right)$$

$$p_1 = 2\left(\frac{2\pi m_h\, kT}{h^2}\right)^{3/2} \exp -\left(\frac{E_t - E_v}{kT}\right) \qquad 2.4.2$$

E = energy level of the trap, E = level of the bottom of the conduction band, E = level of top of valence band, m_e = effective mass of electron, m_h = effective mass of hole, and h = Planck's constant.

The lifetimes can be expressed as

$$\tau = \frac{1}{\langle v\sigma \rangle N_t} \qquad 2.4.3$$

where v = the thermal velocity, σ the capture cross section and N_t = the density of recombination centers. If the capture cross section is assumed independent of temperature, $\tau \propto (\text{velocity})^{-\frac{1}{2}} \propto T^{-\frac{1}{2}}$. Generally one of the terms in the denominator of 2.4.2 predominates so that the generation rate is of the form

$$g = \text{constant} \times T^2 \exp(-\epsilon/kT) \qquad 2.4.4$$

where ϵ = activation energy or separation of trap level and band edge. It is customary to assume that activation energy follows the relation

$$\epsilon = \epsilon_0 + \gamma T \qquad 2.4.5$$

ϵ_0 being the value at absolute zero and γ some constant.

If intrinsic generation occurs within the space-charge region the generation rate will be (Shockley 1949)

$$g = (\text{constant})\,\frac{n_i^2}{\tau} \qquad 2.4.6$$

From Conwell (1952),

$$n_i = 9.3 \times 10^{31} T^3 \exp(-8700/T)\,\text{cm}^{-3} \qquad 2.4.7$$

so, for intrinsic generation

$$g = (\text{constant})T^{\alpha} \exp(-\epsilon_{o\alpha}/kT) \qquad 2.4.8$$

where α is an exponent depending upon the temperature dependence of τ .

Now for a pnp transistor under conditions of double-depletion as in fig. 9c we make the assumption that all the holes generated within the depleted region are carried either to the emitter or collector and that this space charge generated current predominates over current which arises from holes generated within the undepleted region adjacent to the space-charge region. Then

$$I_b = I_e - I_c = g(\text{volume of space charge}) \qquad 2.4.9$$

If generation is through recombination centers the slope of a ln I_b vs 1/T plot will be from 2.4.4

$$s = -\epsilon_o/k - 2T \qquad 2.4.10a$$

and if intrinsic generation predominates the slope will be

$$s = -\epsilon_{o6}/k - \tfrac{7}{2}T \qquad 2.4.10b$$

LOGARITHM OF BASE CURRENT VS 1/T

(Transistor no. 46)

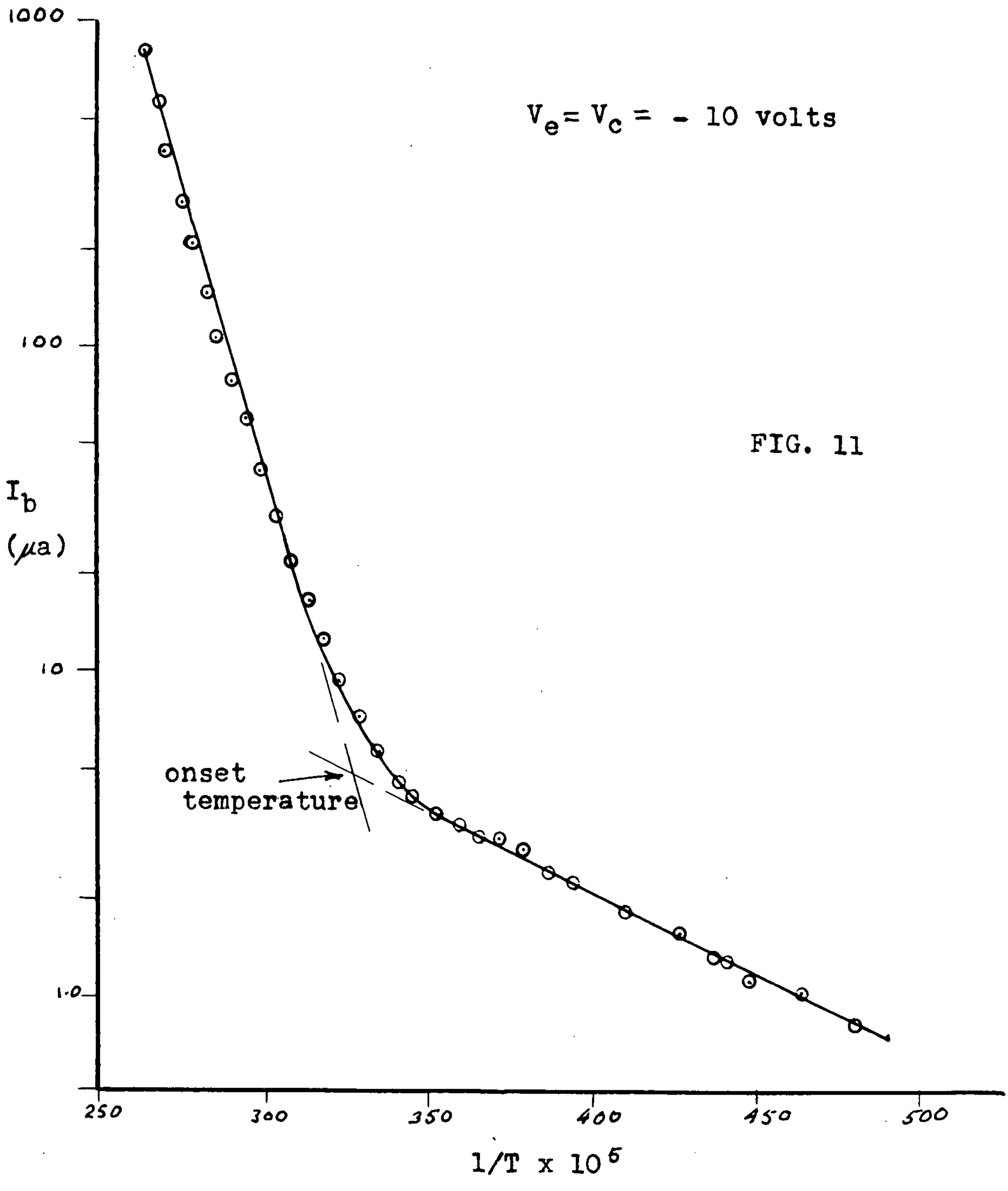

FIG. 11

Base currents were measured in double depleted transistors over a range from 90°C to -60°C. The emitter and collector leads of the specimens were joined and the junctions reverse biased sufficiently to cause a large overlap of the two space charge regions as in fig. 9c. This condition is assured by making the reverse bias equal to or larger than V_p.

For measurements above room temperature the transistor was placed in a heated oil bath and readings were taken as the bath cooled. For measurements below room temperature the oil bath was frozen in a mixture of dry ice and acetone, and readings taken as the bath warmed. A mercury thermometer was used above room temperature and an alcohol thermometer below; in both cases a copper strip provided a thermal connection between the thermometer and the base lead. Temperature rise in the base due to power dissipation is not serious. A typical dissipation constant in air is 0.6°C/mw; at an extreme of 200 μa and 10 volts the temperature rise would be appreciably less than 1.2°C due to the cooling provided by the base fin and oil bath.

The voltage drop between the base and collector-emitter was kept constant by adjustment of the power supply.

A typical plot of log I_b vs 1/T is shown in fig. 11. The activation energies indicated by the upper slopes of the curves ranged from 0.70 ev. to 0.61 ev. The value of

ϵ_{oG} is 0.785 ev. (Conwell 1958), hence it is concluded that the currents at these temperatures do not arise from intrinsic generation but from generation through recombination centers.

One wonders if intrinsic generation might begin to predominate at a temperature above 90°C. A theoretical estimate of "onset temperature", the temperature at which intrinsic generation dominates may be made if it is assumed that this occurs when the majority carrier concentration $n = 2N_D$ where N_D is the donor density.

Using the mass action law

$$n_i^2 = pn \qquad 2.4.11$$

and the charge balance

$$n - p = N_D \qquad 2.4.12$$

one obtains

$$n_i^2 = 2N_D^2 \qquad 2.4.13$$

when $n = 2N_D$. Using equation 2.4.7 for n the onset temperature can be obtained for a given N_D. For specimens studied these temperatures ranged between 60 and 80°C. It is therefore concluded that intrinsic generation does not occur at all in the units used in this investigation.

2.5 Comparison of Space charge Generated and Diffusion Currents.

In making the analysis of activation energies in the

MODEL FOR COMPARISON OF DIFFUSION AND SPACE CHARGE GENERATED CURRENTS

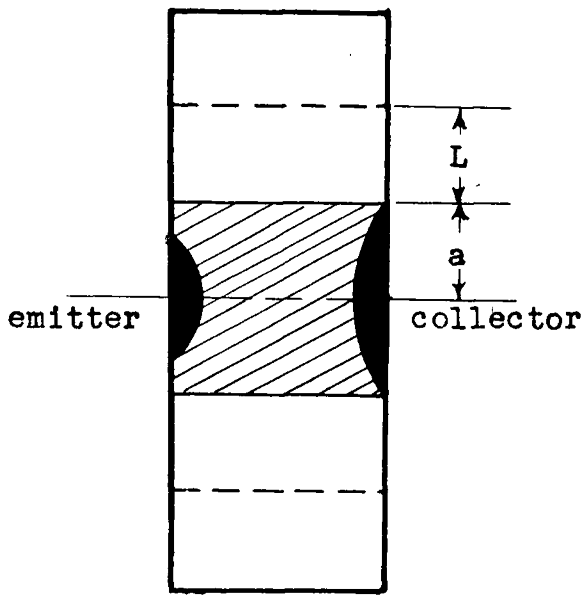

FIG. 12

preceeding section it was assumed that space charge-generated current predominated over diffusion current. This assumption will now be tested analytically following a method of Sah, Noyce and Shockley (1952). Several assumptions regarding physical and geometrical quantities must be made, and to be consistent all will be chosen to make the space-charge-generated current a minimum.

The model in fig. 12 represents the same physical conditions as that of fig. 9c only it is assumed that the overlapping space-charge regions form a cylindrical column between the emitter and collector. The cross-section of the column is chosen as the circular area of the collector. As discussed in section 1.4, the diffusion current consists of, on the average, all the minority carriers generated within one diffusion length L of the space-charge region.

The electron and hole lifetimes τ_{po} and τ_{no} are assumed equal and the trap level is assumed to fall at the intrinsic Fermi level. From equation 1.4.4 the generation rate in the space charge region then has its minimum value of

$$g_{s.c.} = \frac{n_i}{2\tau} \qquad 2.5.1$$

and from 1.4.2 the generation rate in the undepleted n-type region is

$$g_d = \frac{p_o}{\tau} \qquad 2.5.2$$

Multiplying the generation rates by the appropriate volumes calculated from fig. 10 gives the ratio of the space charge-generated and diffusion currents:

$$\frac{I_{s.c.}}{I_d} = \frac{n_o}{2n_i} \cdot \frac{a^2}{L^2 + 2aL} \qquad 2.5.3$$

At temperatures above 300°K, n_o is of the order of N_D or $10^{14}cm^{-3}$, n_i is $2.5 \times 10^{13}cm^{-3}$ at 300°K, and a is about 0.05 cm for the transistors used. The diffusion constant D may be obtained from the mobility of holes in germanium, μ_p = 1800 cm volt sec and the Einstein relation

$$D_p = \mu_p \frac{kT}{q} \qquad 2.5.4$$

The diffusion length is then given by

$$L = \sqrt{D\tau} \qquad 2.5.5$$

It is necessary to make an assumption regarding the lifetime. If following Sah, Noyce and Shockley, we assume $\tau = 10^{-6}$sec, then $L = 7 \times 10^{-3}$cm $\ll$ a and $I_{s.c.}/I_d \simeq 7$. For $\tau = 10^{-5}$sec, $I_{s.c.}/I_d \simeq 2.2$, and for $\tau = 10^{-7}$sec, $I_{s.c.}/I_d \simeq 22$. It is concluded that the assumption that space charge-generated current predominates is a reasonable one.

LOW TEMPERATURE INCREASE IN BASE CURRENT

$V_e = V_c = \text{constant}$

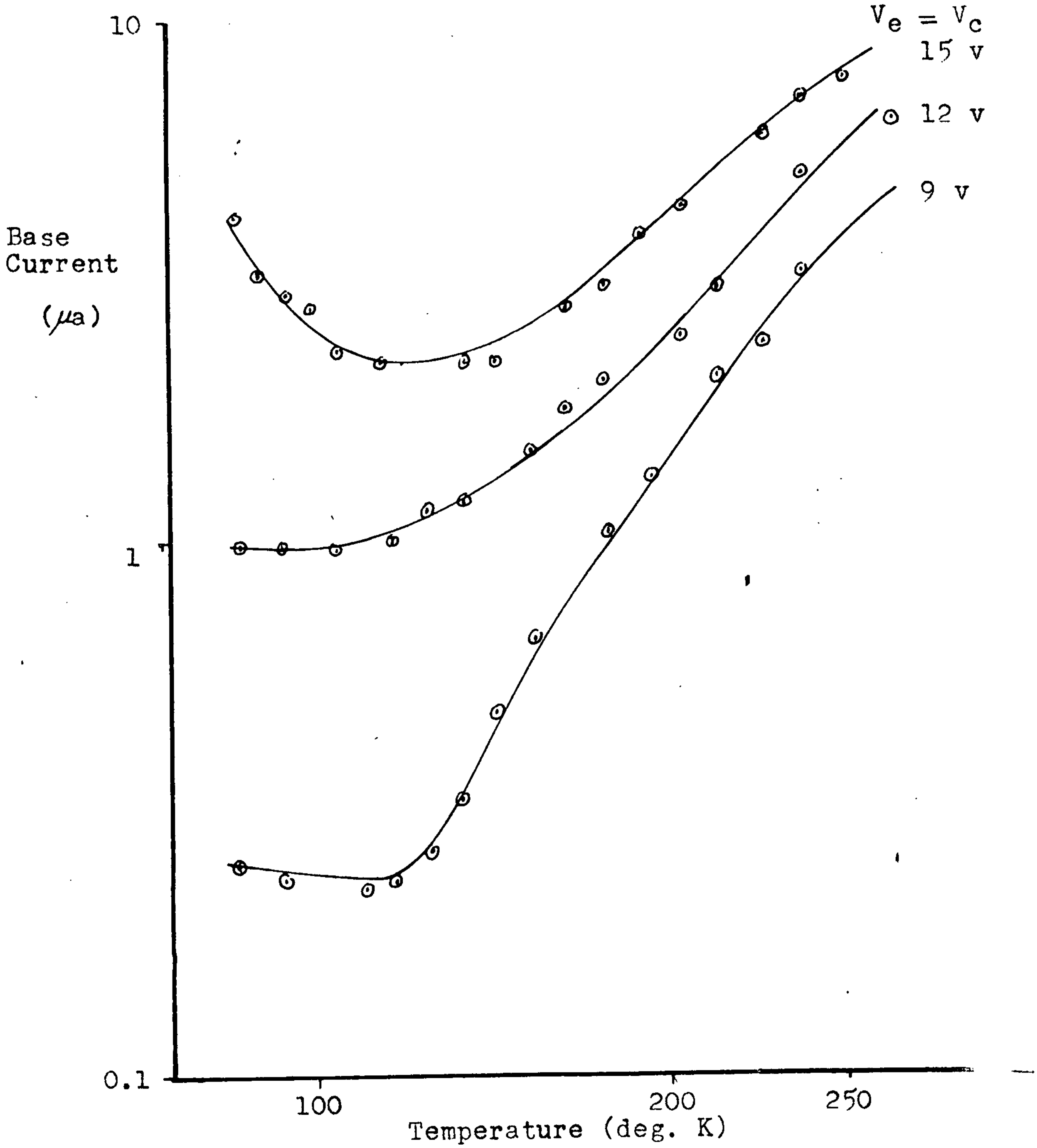

FIG. 13

2.6 Anomalous Behaviour at Low Temperatures

An anomaly was revealed when the measurements of section 2.4 were extended to 190°C by freezing the oil bath in liquid nitrogen. Three specimens exhibited an increase in current with decreasing temperature below a certain temperature. The curve of fig. 13 illustrates this for transistor no. 20, a 2N137 unit. All the units showing this anomaly possessed very low breakdown voltages and "soft" breakdown characteristics.

This phenomena cannot be accounted for by the Shockley-Read theory of recombination and generation via recombination centers. The net generation rate given by equation 1.4.1 must always decrease with temperature; this is shown for the case of generation within the space charge region if we take τ_n, $\tau_p \propto T^{-\frac{1}{2}}$. Then equation 1.4.2 is of the form

$$g_{s.c.} \equiv \frac{\text{Constant } T \exp(-\epsilon_G/kT)}{\text{const}T\exp-(E_c - E_t/kT) + \text{const. } T \exp-(E_t - E_v/kT)} \qquad 2.6.1$$

This is clearly a monotonically increasing function at all temperatures; the same is true for the more general case given by eqn. 1.4.1.

These results are similar to an anomalous increase in carrier concentration at low temperatures observed in heavily doped silicon p-type specimens by Pearson and

Bardeen. These results were associated with degeneracy of electrons in the conduction band. It is worth considering whether the anomalous results in the present case may not be caused by degeneracy resulting from avalanche multiplication of carriers in the base.

The required density of electrons in the conduction band for degeneracy to occur at a given temperature is, from Shockley (1949)

$$n_{deg} = 3.7 \times 10^{15}\left(\frac{m_n}{m}\right)^{\frac{3}{2}} T^{\frac{3}{2}} \qquad 2.6.3$$

where m_n = effective mass of electron, about 0.5 m for intrinsic germanium (Conwell 1958). For no. 20 the current increase occurs at 120°K for which $n_{deg} = 2 \times 10^{18}$cm. is required. However, the concentration of electrons that would occur in the absence of breakdown is

$$n = \tfrac{1}{2}(N_D - \sqrt{N_D^2 - 4n_i^2}) = N_D \qquad 2.6.4$$

as $N_D \gg n_i$. Thus at 120°K, $n = 10^{14}$cm. so a multiplication factor of 10,000 is required. The avalanche multiplication factor as defined by

$$I = MI_{saturation} \qquad 2.6.5$$

is only about 10 at 15 volts reverse bias, room temperature. Thus it is concluded that degeneracy is not responsible for the anomaly.

CHAPTER III

ORIGIN AND DISTRIBUTION OF REVERSE CURRENTS UNDER CONDITIONS OF DOUBLE-DEPLETION

3.1 Current Distribution under Conditions of Double-Depletion

The distribution of current in an ideal transistor under conditions of double-depletion may be obtained directly from the Shockley equations (1.3.1 and 1.3.2). However, there are several factors which will cause the current distribution in a real transistor to deviate from that predicted by theory: design practice is to make the collector area several times that of the emitter in order to improve; there may be unequal impurity density throughout the base material; and avalanche multiplication may occur at one or both junctions.

The simplest modification of the Shockley equations which takes into account unequal electrode areas is the replacement of the common area A for the collector and emitter by the differing areas A_e and A_c. The equations then become, for a pnp transistor,

$$I_e = \frac{p_n q\ D_p}{L_p}\left[A_e \operatorname{csch}\frac{W}{L}\left(e^{\frac{qV_e}{KT}}-1\right) - A_c \coth\frac{W}{L}\left(e^{\frac{qV_c}{KT}}-1\right)\right] \quad 3.1.1$$

$$I_c = -\frac{p_n q\ D_p}{L_p}\left[A_c \operatorname{csch}\frac{W}{L}\left(e^{\frac{qV_c}{KT}}-1\right) - A_e \coth\frac{W}{L}\left(e^{\frac{qV_e}{KT}}-1\right)\right] \quad 3.1.2$$

For the situation in which the collector is floating and the emitter is reverse biased to saturation, ie $I_c = 0$, we have

$$I_{eo} = - \frac{p_n q\ D_p}{L_p} A_e \tanh\left(\frac{W}{L}\right) \qquad 3.1.3$$

and, similarly, when the collector is biased to saturation and the emitter is floating

$$I_{co} = + \frac{p_n q D_p}{L_p} A_c \tanh\frac{W}{L} \qquad 3.1.4$$

the ratio of the reverse saturation currents is then

$$\frac{I_{eo}}{I_{co}} = - \frac{A_e}{A_c} \qquad 3.1.5$$

as for an ideal transistor.

Another situation of interest is that for which both junctions are reverse biased to saturation but not to so high a voltage that the effective base width is significantly decreased by expansion of the space charge regions. For this case we have

$$I_e = \left[- A_c \operatorname{csch}\frac{W}{L} + A_e \coth\frac{W}{L}\right] \frac{q\ p_n D_p}{L_p} \qquad 3.1.6$$

and

$$I_c = \left[+ A_e \operatorname{csch}\frac{W}{L} - A_c \coth\frac{W}{L}\right] \frac{q\ p_n D_p}{L_p} \qquad 3.1.7$$

The ratio of these currents is

$$\frac{I_e}{I_c} = \frac{- A_c \operatorname{csch}\frac{W}{L} + A_e \coth\frac{W}{L}}{A_e \operatorname{csch}\frac{W}{L} - A_c \coth\frac{W}{L}} \qquad 3.1.8$$

$$\simeq \frac{(A_c - A_e) - \frac{W^2}{6L^2}(2A_e + A_c)}{(A_c - A_e) + \frac{W^2}{6L^2}(2A_c + A_e)}, \quad \text{for } w \ll L$$

REVERSE CURRENT-VOLTAGE CHARACTERISTIC

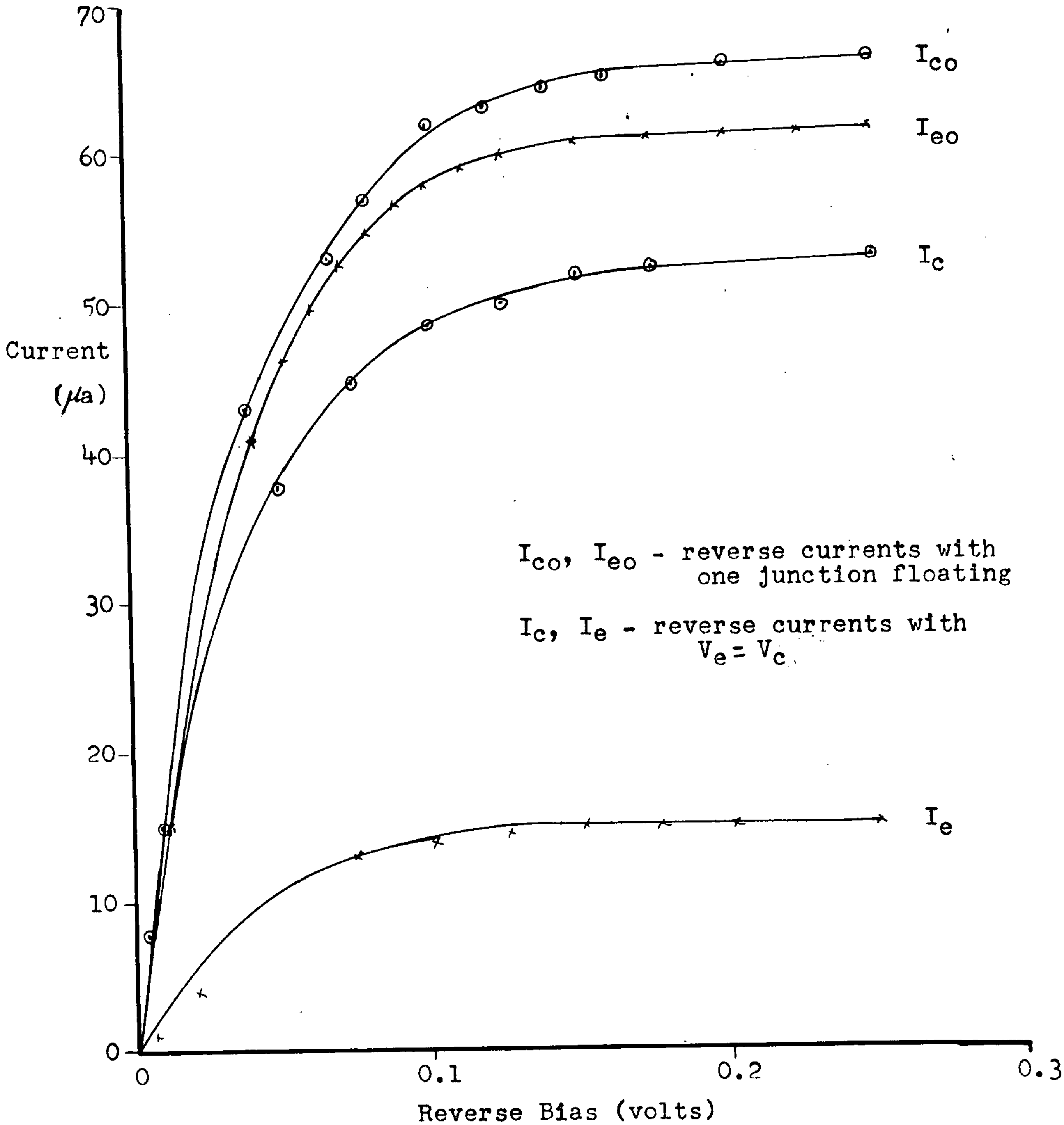

FIG. 14

Experimental measurements of the currents described above were made for two transistors and a typical curve is illustrated in fig. 14. The ratio I_{eo}/I_{co} is only -1.07 implying, contrary to fact, that $A_e > A_c$. The ratio of the saturation currents when both junctions are reverse biased is $I_e/I_c = -0.28$. The largest value of A_c/A_e for which the ratio of equation 3.1.8 is possible is about 3.6 and this happens for the case that $w > L$, whereas in fact L is larger than w for the units tested.

The simple modification of the Shockley equation introduced is thus unsatisfactory since it leads to inconsistencies in the choice of the parameters w/L and A_c/A_e to disagreement with the values of A_c and A_e obtained by capacity measurements. We therefore conclude that the other factors mentioned at the beginning of the section are important in determining the distribution of reverse currents in the units tested.

As the regulation of the reverse current at one junction by variation of the reverse current at the other will be discussed in section 3.3, it is of interest to note that for the typical unit of fig. 14, the collector saturation current can be varied over a range of 13μa by varying the emitter bias, while the emitter current can be varied 49μ a by varying the collector reverse bias.

3.2 Non-saturating Reverse Currents

It has been shown in Section 2 that the reverse current at a junction arises mainly from carriers generated in the space-charge region. To determine whether the non-saturating of the reverse current can be ascribed to expansion of the space charge region an experimental situation must be chosen for which the volume of the space charge region can be related to the applied bias. For a transistor in which the collector and emitter are hemispheres of p-type material extending into the base, this may be arranged by applying an equal reverse bias to the emitter and collector of such a value that the two space charge regions overlap to form a cylindrical column of space charge extending outwards into the base wafer. The volume of this space-charge region may then be obtained by an integration of Poisson's equation in cylindrical co-ordinates with suitable boundary conditions. This is carried out in the Appendix with the result, in mks units,

$$V - V_m = \frac{\rho R^2}{4\epsilon}\left(1 - \frac{a^2}{R^2} + \frac{a^2}{R^2}\ln\frac{a^2}{R^2}\right) \qquad 3.2.1$$

where V is the reverse bias, V_m the minimum reverse bias at which cylindrical geometry can be applied (i.e. at which the region directly between the junctions is just depleted), R the radius of the cylinder at the latter voltage, and a the radius of the cylinder for $V > V_m$.

Now, the space-charge generated current is directly proportional to the volume of the space charge region which is in turn directly proportional to ^{2}, so equation 3.2.1 may be written

$$V - V_m = \frac{\rho R^2}{4\epsilon}\left(1 - \frac{I}{I_m} + \frac{I}{I_m}\ln\frac{I}{I_m}\right) \qquad 3.2.2$$

where I is the base current, that is, the total reverse current across the emitter and collector junctions, and I_m is the base current at $V = V_m$. For $\left|\frac{I}{I_m} - 1\right| \ll 1$, this may be approximated as

$$V - V_m = \frac{\rho R^2}{8\epsilon}\left(\frac{I - I_m}{I_m}\right)^2 \qquad 3.2.3$$

which is the equation of a parabola.

To fit experimental values of V and I to the curve of equation 3.2.3 one can estimate V_m and take I_m as the experimental value of I at this point. The constant $\frac{\rho R^2}{4\epsilon}$ may be used as a parameter and chosen to make the theoretical curve coincide with one experimental point. The other experimental points will lie along the curve if the excess current does arise from the expansion of the space charge region.

Base current as a function of bias voltage was measured for several transistors at 50°C and at room temperature. The results for all except one unit proved unsuitable for comparison with theory because of early breakdown or high punchthrough voltage. In the latter case it was thought that the formation of a cylindrical space charge region did

REVERSE CHARACTERISTIC SHOWING INCREASE IN SATURATION CURRENT

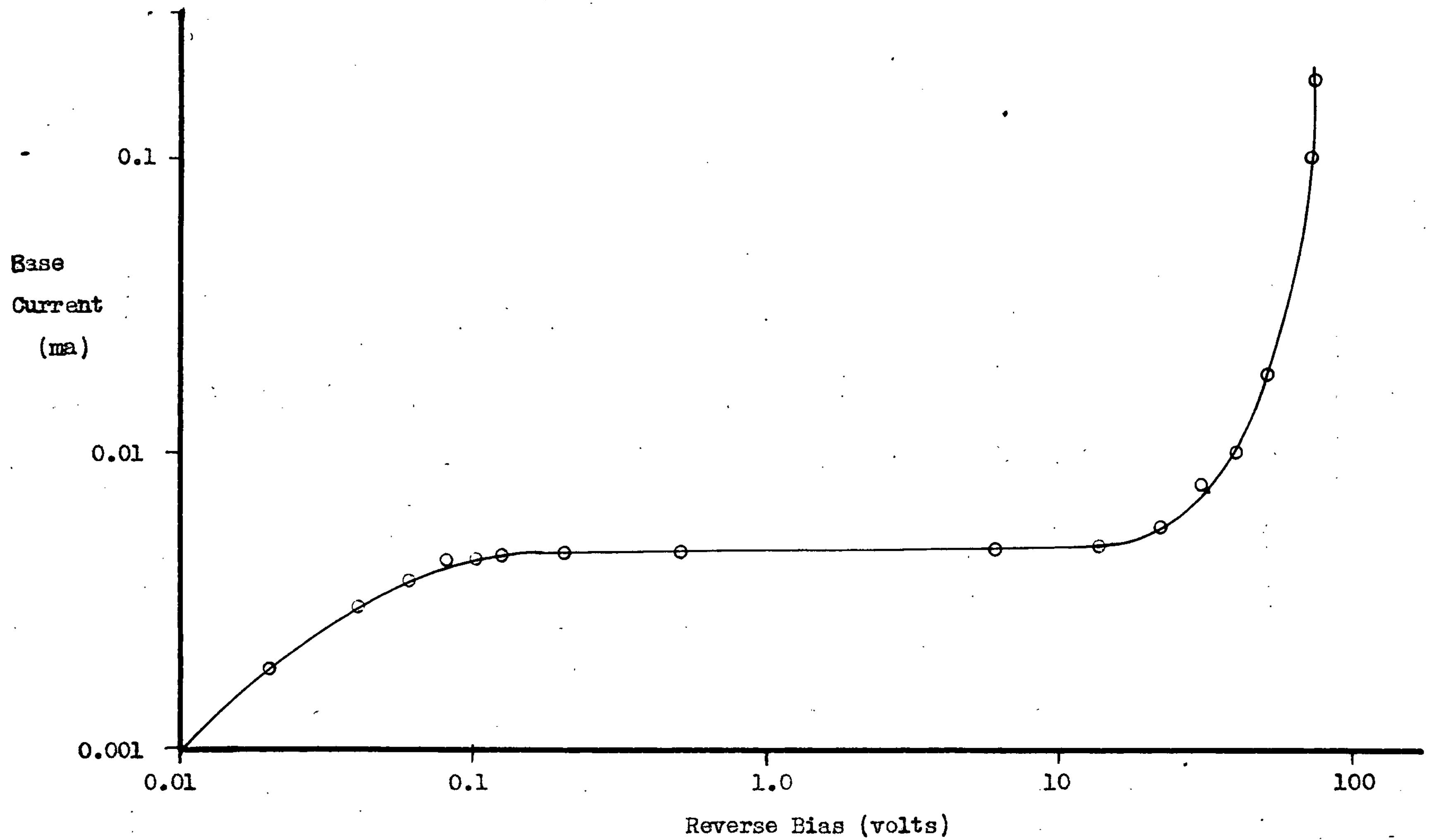

FIG. 15

not occur until the reverse-bias was in the region of breakdown.

The current-voltage characteristic for transistor No. 39, a 2N137 unit, is illustrated in fig. 15. The value of V_m was taken to be $V_p/4$, the value of V at which the two space charge regions would meet in an ideal planar transistor. Because of the very small increase in current over the range between V_m and breakdown, it was practical to take only three points from the experimental curve. The constant was chosen such that the theoretical curve passed through the experimental point having the lowest value of V. It will be seen from fig. 16 that the agreement of the two other experimental points is very good.

From this fit the following numerical information is obtained:

$$\frac{\rho R^2}{\epsilon} = 8.9 \times 10^4 \text{volt}$$

which is consistent with $\rho = 50$ coul.m^{-3} ($N_D = 3 \times 10^{14}$ cm^{-3}), $R = 0.5 \times 10^{-3}$m., $\epsilon = 1.4 \times 10^{-10}$F.m.$^{-1}$ which are reasonable values for the structure examined.

3.3 Operation of Transistors as Amplifiers under Conditions of Double-Depletion

The findings of Stafayev et al (1956) mentioned in the introduction indicate that a transistor may be operated practically as an amplifier under conditions of double-depletion. It is worth while to review here the simple

COMPARISON OF I_b/I_m VS $V - V_m$ WITH THEORETICAL CURVE FOR CYLINDRICAL EXPANSION OF THE SPACE CHARGE REGION

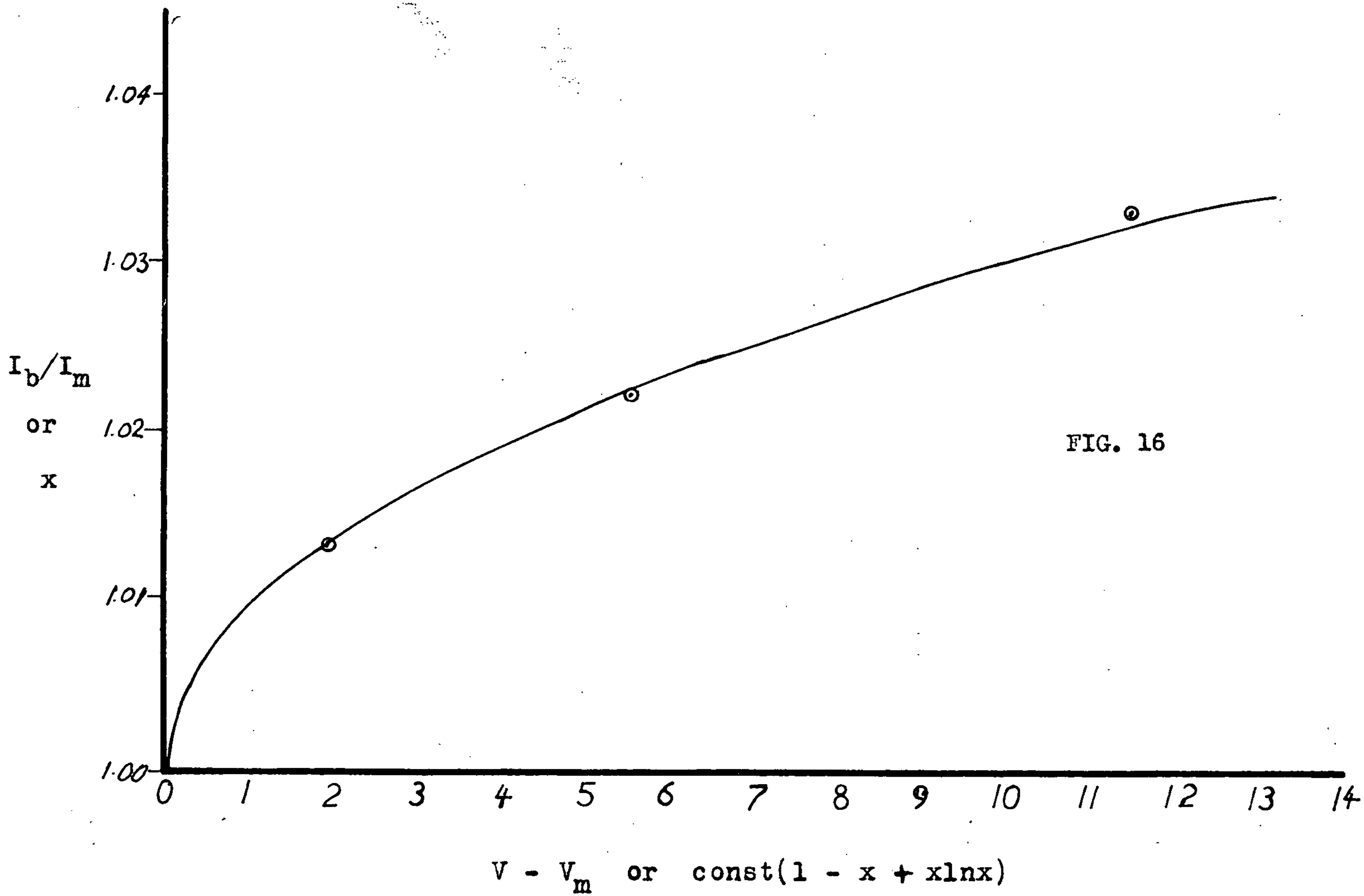

FIG. 16

principles of operation of such a device, especially as the results of section 3.1 indicate that such operation is possible for the units investigated.

A germanium pnp transistor conventionally biased as an amplifier acts on an injection system described as follows

$$I_c = I_{co} + \alpha I_e \qquad 3.3.1$$

where I_{co} is the saturation current across the collector junction when the emitter is unbiased and is the grounded base current amplification factor. In a system of double depletion the relation becomes

$$I_c = I_{co} - \alpha|I_e| \qquad 3.3.2$$

This relation obtains only when the base width is of the order of L; then the two space-charge regions are to some extent interacting for the boundaries of the regions are not sharp in a real transistor. Under this condition one electrode may draw carriers not only from the undepleted region of the base but also by a "robbing" action from the space charge region of the other electrode.

The two electrodes will be referred to as the control electrode and the collector. Amplification becomes possible with asymmetry of the working of the control electrode and the collector which can be achieved by a dissimilar geometry or by application of different bias values. The bias value on the collector must be great enough to assure operation in the collector saturation region. Amplification will occur until the control electrode current becomes saturated. Since I_{co} is small in Ge transistors except at high temperatures it is only practical to use them as reverse-biased amplifiers at high temperatures.

The Russian investigators made measurements on pnp germanium transistors using the electrode with the larger area as the control electrode. Measurements of current and power amplification with grounded control electrode as in fig. 17(a) were made at various temperatures with both forward and reverse biases on the control electrode. Small signals were used at a frequency of 1000 cps. Some of the results from the Russian paper are shown in fig. 17.

When the control electrode is forward biased, the amplifier circuit is equivalent to the grounded emitter configuration so the current amplification factor will be referred to as β. For the transistors used by the Russians, I_{co} was about 2 ma at 100°C. and 1 ma at 81°C. as shown in fig. 17 (b), (c). Under double-depletion conditions, they achieve a maximum current amplication of 13 db and a power amplification, g, of 26 db at an operating temperature of 81°C. The maximum collector current is of course limited to I_{co}.

An important feature of these curves is the displacement of the maximums of β and g into the region of negative currents at higher temperatures. As pointed out by the Russians this appears to contradict the generally accepted

WORKING OF A TRANSISTOR UNDER CONDITIONS

OF DOUBLE-DEPLETION

(After Stafeyev, et al)

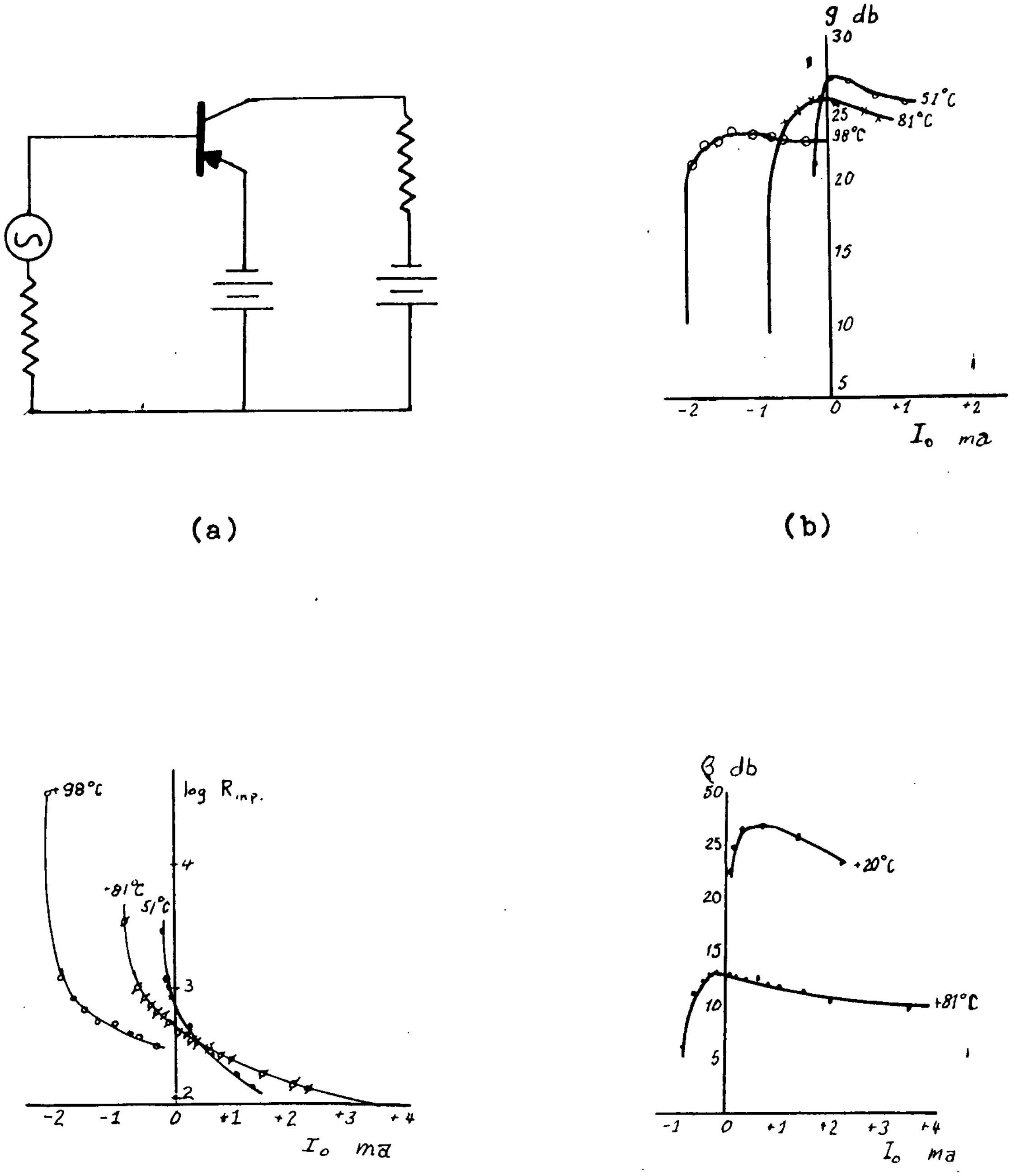

FIG. 17

explanation for the maximum in β due to Webster (1954) which asserts that the fall-off of β at low reverse biases is owing to the increased effect of surface recombination at low fields, while the decline at higher values of I_e is caused by decreased emitter efficiency. The results of our own investigation can be utilized to explain this anomaly. As deduced from the curve of fig. 11 surface recombination and generation are negligible at higher temperatures; therefore there would be no apparent decrease in β as I_e approaches zero. The decline which occurs with increasing reverse bias is caused by saturation of the control electrode current. This reasoning is supported by the fact that the sharp decreases of to zero in the Russian results occurs at collector currents of about the value of I_{co}.

The Russian investigators note that, for specimens tested with the smaller electrode as control electrode there was a displacement of the maximum of β in the direction of lower I_e but it remained in the injection region. In this case saturation of the control electrode occurs at a lower current and does not attain its maximum until I_e is positive.

Fig. 17 (d) shows the relation of the input resistance to the current of the control electrode. When the control electrode current is far from saturation, the input resistance is much smaller than the output resistance (about 50 ohms) so that voltage amplification is also possible.

The transistors used in the present investigation would not be suitable for use as reverse biased amplifiers because of their relatively low saturation currents up to 100°C. With appropriate geometry and doping, however, transistors might be made which utilize the advantages of the double-depletion system: higher power amplification at high temperature and stable power amplification with variation in temperature.

CHAPTER IV

DISCUSSION OF BREAKDOWN VOLTAGES

In the course of this investigation breakdown voltages were measured for the purpose of selecting suitable specimens for the main experimental work. These measurements will now be discussed in the light of existing theory for breakdown at p-n junctions.

Breakdown voltage was defined for purposes of measurement as that value of the reverse bias across a junction at which the reverse current has increased to 5 times its saturation value. This criterion is unsatisfactory in that it does not take into account the increase of current with voltage, and it is possible that a relatively slow increase in current due to the non-saturating of reverse current rather than a sharp increase due to avalanche breakdown may cause an increase to 5 times the value of the saturation current. One such factor leading to non-saturation of the reverse current has been discussed in Chapter III, another of importance is a large recombination-generation rate on the surface of the base in the vicinity of the emitter and collector regions. As the space-charge region around the emitter or collector expands, more of the surface contributes to the minority carrier flow into the base.

For all specimens tested, the breakdown voltage as defined above was much lower than the bulk breakdown voltage calculated using Miller's formula (equation 2.1.2) and estimates of impurity density obtained as in section 2.1. For instance, for the transistors described in Table 1, the measured breakdown voltages were 12, 17 and 30 v compared to calculated bulk values of 328, 795 and 608 respectively.

As pointed out in the introduction, breakdown may occur between the surface and the space-charge region of the bulk, therefore the results obtained were examined to find if there was any correlation between the measured breakdown voltages and the floating emitter and surface conductance measurements obtained as described in section 2.2. No regular increase or decrease of breakdown voltage with surface conductance or floating emitter voltages was found.

The only theory available for surface breakdown is that of Garrett and Brattain (1956) which is based on a one-dimensional model. They obtain a relation between surface breakdown voltage, bulk breakdown voltage and impurity density as follows

$$V_{bulk} - V_{surf.} = \frac{2\pi e \sigma^2}{n_i \epsilon \epsilon_0 N_I \mu} \qquad 4.1$$

where σ is the surface charge density, ϵ the semiconductor dielectric constant, N_I the impurity density and n_i the minority carrier density.

This relation cannot readily be applied to the experimental data because of the uncertainty in σ . Not only is its value uncertain, but it is very likely that it is dependent on such factors as the reverse bias and the impurity density.

CHAPTER V

SUMMARY

This work has been concerned with an investigation of space-charge regions in germanium by utilization of the double-depletion condition. Experimental data have been discussed in terms of specific geometrical and physical models for carrier generation processes.

In Chapter II methods of obtaining indirectly the electronic and geometrical parameters of junction transistor structures are described. A cylindrical three-dimensional model under the condition of double-depletion is described and it is shown that, adopting the Shockley-Read recombination-generation theory, the minority carrier current flowing in the base arises predominantly in the space charge region and not by diffusion from the neutral region of the bulk.

Experimental data between 100°C and -190°C have been analysed and activation energies of carriers derived by application of the Shockley-Read theory. It was further deduced that two sets of recombination-generation centers are active; the set having the higher activation energy was ascribed to bulk impurities and the lower to surface states. It was deduced that intrinsic generation of carriers does not contribute to the hole flow in specimens investigated, even at very high temperatures.

Some specimens showed an anomalous increase in current at low temperatures which could not be accounted for by the Shockley-Read theory or by degeneracy of electrons in the conduction band at low temperatures. It is conjectured that some unknown surface generation mechanism may account for this unusual behaviour.

In Chapter III the current distribution between the two junctions when both are reverse-biased is discussed. It is deduced from experimental data that the current distribution is roughly in proportion to the area of the junctions when both are equally reverse-biased. The generation rate of carrier pairs per unit volume will be the same in the two depletion regions and the current flow to the junctions will therefore be proportional to the volumes of the regions and hence approximately proportional to the junction areas.

It was further found that interaction between reverse-biased junctions separated by less than a diffusion length becomes significant at elevated temperatures. This is related to the ability of each junction to receive (by diffusion) carriers from the space-charge region around the other junction and consequently ($\partial I_e / \partial I_c$) is not negligible compared with unity under these conditions. A discussion is included of the proposal of Stafayev, Tuchkevich and Yokovchuk for the use of junction transistors as amplifiers at high temperatures under conditions of double-depletion.

It is shown that the phenomena of non-saturating reverse current can arise from expansion of the space charge region into the base. A relation relating the base current and the reverse bias at the junction is developed for a cylindrical model assuming that the rate at which carriers are generated in the space charge region greatly exceeds that at which carriers diffuse into it from the undepleted region. The theoretical current-voltage relation is shown to give a very good agreement with the experimental data for one specimen.

MODEL FOR CYLINDRICAL EXPANSION

OF THE SPACE-CHARGE REGION

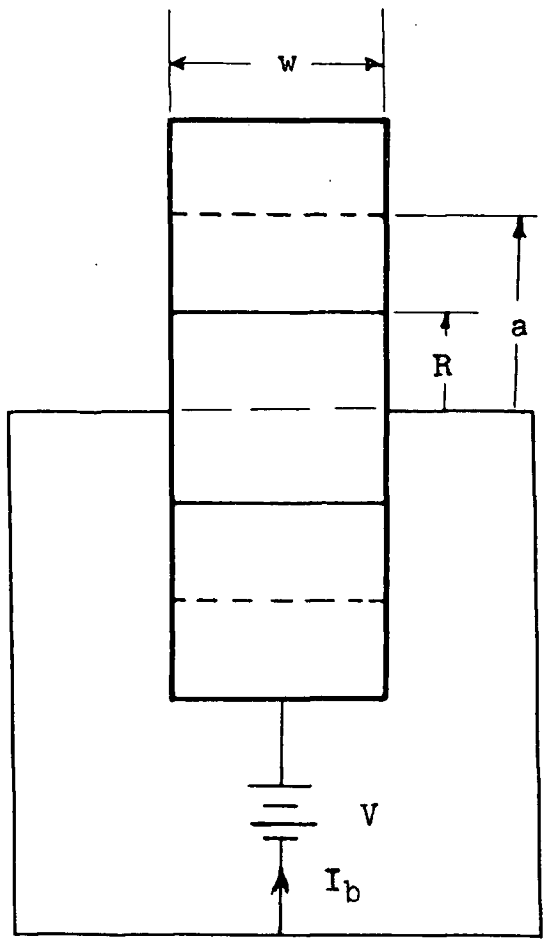

R = radius of space-charge region at $V = V_m$

FIG. 18

APPENDIX

DEPENDENCE OF THE VOLUME OF A CYLINDRICAL SPACE CHARGE REGION ON REVERSE BIAS

When a transistor consisting of hemi-spherical p-type emitter and collector extending into an n-type base wafer is biased as shown in fig. 17, then at some value of reverse bias, $V - V_m$, the space charge regions of the emitter and collector will overlap to form a cylindrical column of space-charge of length w and radius R. For $V > V_m$ the extent of the space charge region may be determined by the solution of Poisson's equation in cylindrical co-ordinates.

For the case of radial symmetry and constant length as in this situation Poisson's equation becomes,

$$\nabla^2\Psi = \frac{1}{r}\frac{\partial}{\partial r}\left(r\frac{\partial\Psi}{\partial r}\right) = -\frac{\rho}{\epsilon} \qquad \text{A.1}$$

where Ψ is the potential, r the radial distance from the axis, and ρ and ϵ the space charge density and permittivity in mks units. If a is the value of r at the boundary of the space charge region, then the boundary conditions are:

(i) $\left(\frac{\partial\Psi}{\partial r}\right)_a$

(ii) $\Psi(a) - \Psi(R) = V - V_m$

The general solution of equation A.1, valid for $V > V_m$ and $r > R$ is

$$(r) \quad \frac{\rho}{4\epsilon}r^2 + B\ln\frac{r}{R} + C \qquad \text{A.2}$$

where B and C are constants of integration.

Using boundary condition (i)

$$B = \frac{\rho}{2\epsilon} a^2 \qquad \text{A.3}$$

and from boundary condition (ii)

$$\begin{aligned} \Psi(a) - \Psi(R) &= V - V_m \\ &= \frac{\rho}{4\epsilon} R^2 \left(1 - \frac{a^2}{R^2} + \frac{a^2}{R^2} \ln \frac{a^2}{R^2}\right). \end{aligned} \qquad \text{A.4}$$

BIBLIOGRAPHY

Brown, W.L., "N-Type Surface Conductivity on P-Type Germanium", Phys. Rev., 91 (1953), pp. 518-527.

Barker, A.S., "A Study of Space-Charge and Avalanche Multiplication Processes in Germanium", Thesis for Master of Science Degree, University of British Columbia, September, 1957

Christensen, H., "Surface Conduction Channel Phenomena in Germanium", Proc. IRE 42 (1954) pp. 1371-1376.

Conwell, E.M., "Properties of Silicon and Germanium", Proc. IRE, 40 (1952), pp. 1327-1337.

Conwell, E.M., "Properties of Silicon and Germanium: II", Proc. IRE, 46 (1958), pp 1281-1300.

Early, J.M., "Effects of Space-Charge Layer Widening in Junction Transistors", Proc. IRE, 40 (1952), pp. 1401-1406.

Garrett, C.G.B., Brattain, W.H., "Some Experiments on, and a Theory of, Surface Breakdown", J. App. Phys., 27 (1956), pp. 299-306.

Miller, S.L., "Avalanche Breakdown in Germanium", Phys. Rev., 99 (1955), pp. 1234-1241.

McWhorter, A.L., Kingston, R.H., "Channels and Excess Reverse Current in Grown Germanium P-N Junction Diodes", Proc. IRE, 42 (1954), pp. 1376-1380.

Nichol, D.W., "Space-Charge-Limited Currents in Germanium", Thesis for Master of Science degree, University of British Columbia, September 1958.

Sah, C.T., Noyce, R.N., Shockley, W., "Carrier Generation and Recombination in P-N Junction Characteristics", Proc. IRE, 45 (1957), pp. 1228-1243.

Schenkel, H., Statz, H., "Voltage Punch-Through and Avalanche Breakdown and their Effect on the Maximum Operating Voltages for Junction Transistors", Proc. Nat'l Electronics Conf., 10 (1954), pp. 614-625.

Shockley, W., "The Theory of P-N Junctions in Semiconductors and P-N Junction Transistors", Bell Sys. Tech. Jr., 28 July 1949, pp. 435-489.

Shockley, W., "Electrons and Holes in Semiconductors", Van Nostrand, 1950.

Shockley, W., Sparks, M., Teal, G.K., "P-N Junction Transistors", Phys. Rev., 83 (1951), pp. 151-162.

Shockley, W., Read, W.T., "Statistics of Recombination of Holes and Electrons", Phys. Rev., 87 (1952), pp. 835-842.

Shockley, W., "Electrons, Holes and Traps", Proc. IRE, 46 (1958), pp. 973-990.

Stafeyev, V.I., Tuchkevich, V.M., Yakovchuk, N.S., "Operation of a Transistor in Conditions of Depletion", Zh. Tekh. Fiz., 26 (1956), pp. 15-21.

Statz, H., deMars, G., Davis, L., Adams, A., "Surface States on Silicon and Germanium Surfaces", Phys. Rev., 106 (1957), pp. 455-464.

Statz, H., de Mars, G.A., "Electrical Conduction via Slow Surface States on Semiconductors", Phys. Rev., 111 (1958) pp. 169-182.

Webster, W.M., "On the Variation of Junction Transistor Current-Amplification Factor with Emitter Current", Proc. IRE, 42 (1954), pp. 914-920.